Thin Solid Films 519 (2011) 5820–5825

Contents lists available at ScienceDirect

Thin Solid Films

journal homepage: www.elsevier.com/locate/tsf

Effects of physical growth conditions on the structural and optical properties of sputtered grown thin HfO_2 films

Gulnur Aygun [a,*], Ayten Cantas [a], Yilmaz Simsek [a], Rasit Turan [b]

[a] Department of Physics, İzmir Institute of Technology, Gülbahçe Campus, TR-35430 Urla-İZMİR, Turkey
[b] Department of Physics, Middle East Technical University, TR-06531 Ankara, Turkey

ARTICLE INFO

Available online 31 December 2010

Keywords:
HfO_2
Reactive DC sputtering
XPS depth profiling
Spectroscopic ellipsometer
FTIR
XRD

ABSTRACT

HfO_2 thin films were prepared by reactive DC magnetron sputtering technique on (100) *p*-Si substrate. The effects of O_2/Ar ratio, substrate temperature, sputtering power on the structural properties of HfO_2 grown films were studied by Spectroscopic Ellipsometer (SE), X-ray diffraction (XRD), Fourier transform infrared (FTIR) spectrum, and X-ray photoelectron spectroscopy (XPS) depth profiling techniques. The results show that the formation of a SiO_x suboxide layer at the HfO_2/Si interface is unavoidable. The HfO_2 thickness and suboxide formation are highly affected by the growth parameters such as sputtering power, O_2/Ar gas ratio during sputtering, and substrate temperature. XRD spectra show that the deposited films have (111) monoclinic phase of HfO_2, which is also supported by FTIR spectra. XPS depth profiling spectra shows that highly reactive sputtered Hf atoms consume some of the oxygen atoms from the underlying SiO_2 to form HfO_2, leaving Si–Si bonds behind.

© 2010 Elsevier B.V. All rights reserved.

1. Introduction

In order to overcome the scaling limit of conventional Si-based insulators, high permittivity (high-κ) materials are being developed as alternative dielectrics. Having high-κ value around 25 and being thermodynamically stable when grown on Si, HfO_2 is considered to be the most promising candidate to replace SiO_2 [1]. Important film properties including dielectric constant and refractive index of grown thin oxide film depend on the growth parameters [2] as well as the initial thin film constitution [3]. Moreover, the interfacial properties of grown film play crucial role in the electrical properties of the devices [4]. Therefore, it should be noted that the applied physical conditions must be well controlled through the film growth processing steps in order to improve the grown film's dielectric properties.

A number of various film growth techniques have been used to fabricate high-κ materials such as thermal oxidation [5], a variety of chemical vapor deposition techniques [6], ion beam deposition [7], atomic layer deposition [8], pulsed laser deposition [9], laser oxidation [10], remote plasma oxidation [11], DC and RF sputtering [5,12]. Since each method has some advantages and disadvantages, it is not yet clear which method would be the best choice for device applications.

This paper presents reactively grown HfO_2 thin film by DC sputtering technique on *p*-Si (100) substrate with native oxide. The optical and structural characteristics of grown thin hafnium-oxide films were studied with a few characterization techniques in a more detailed manner to understand the effect on the grown film's properties of physical growth conditions.

2. Experimental procedure

HfO_2 thin film was grown on Si substrate by reactive DC magnetron sputtering technique. *p*-type Si (100) substrate with resistivity of 7–17 Ω cm was cleaned chemically in boiling trichloroethylene, acetone with ultrasonic bath, and rinsed with ultrapure water. After drying the wafer with pure N_2 gas, it was mounted onto the substrate holder having a 7.4 cm distance to the target of magneto sputtering deposition chamber vacuumed with a Turbo Molecular Pump (TMP). A 2" diameter with 0.25" thick of 99.9% pure hafnium target was used. It was pre-sputtered for 3 min with Ar gas to remove the possible surface contamination of target. 30 sccm Ar gas flow was used for all processes. In order to get the required gas ratio, i.e. O_2/Ar, oxygen gas flow was changed correspondingly. Base pressure of sputtering chamber was below 2×10^{-6} Torr while working pressure during the sputtering was 0.44×10^{-3} Torr. Prior to, as well as during deposition, the substrate was heated by a halogen lamp and the substrate's temperature was adjusted by a temperature controller. Sputtering time duration was 5 min for the growth processes. Thin film deposition rate can be controlled by both the DC source and gas flow level of reactive O_2 and Ar gas mixture (Fig. 1).

Spectroscopic Ellipsometer (SE) measurement of thin HfO_2 film on *p*-Si (100) was made in the wavelength range of 300–850 nm with an in-situ Sentech SE-801. In-situ SE measurement at 70° incident light beam on the sample surface was realized to obtain the characteristic parameters obtained by SE, i.e. DELTA and PSI. SpectraRay program

* Corresponding author.
E-mail address: gulnuraygun@iyte.edu.tr (G. Aygun).

0040-6090/$ – see front matter © 2010 Elsevier B.V. All rights reserved.
doi:10.1016/j.tsf.2010.12.189

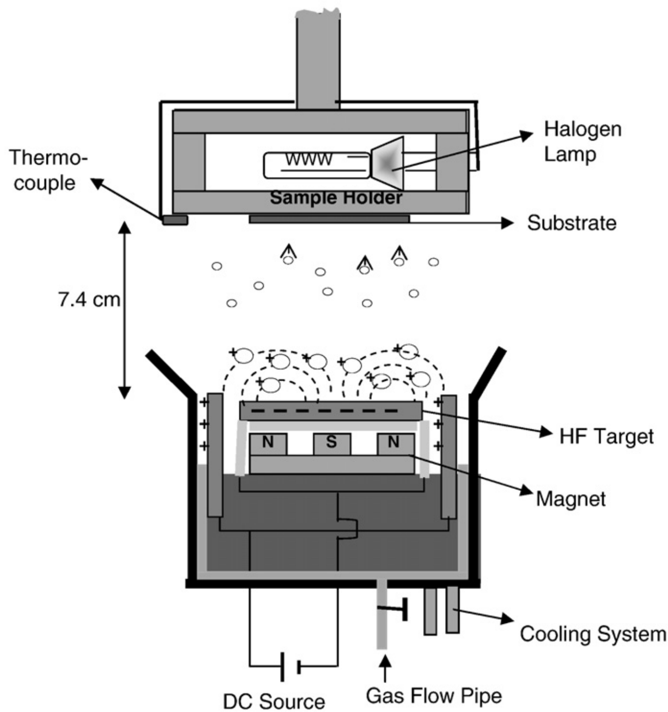

Fig. 1. Inside view of the sputtering chamber with sample holder used for DC sputtering method.

was used for modeling and fitting processes of the SE data from the wavelength range from 350 to 850 nm. The outcomes of this process were refractive index (n), thickness (d), absorption (κ) and transmission of measured film.

Chemical composition and the structure of oxide films were examined by a FTIR spectrometer (BRUKER Equinox 55). X-ray diffraction (XRD) pattern was measured by a Rigaku Miniflex system equipped with CuK_α radiation of average wavelength 1.541 Å. The XRD pattern was analyzed in terms of observed peak positions at specific 2θ values and relative intensities of the peaks by means of a computer software equipped with an ICDD database.

X-ray Photoelectron Spectroscopy (XPS) measurements were realized with a SPECS EA200 (Electron Spectroscopy for Chemical Analysis) system equipped with a hemispherical electron analyzer at a take off angle of 90°. Excitation source was monochromatic AlK_α line with a power of 490 W. The pressure was 7.5×10^{-10} Torr. The film surface was sputtered by Ar^+ ions having the energy of 2000 eV with totally 19 etching cycles (etched layer numbers) each lasted for 3 min. XPS measurements were done with 96 eV pass energy and 0.1 eV step size. Binding energies were corrected with respect to C 1s peak at 284.6 eV and Si 2p peak at 99.3 eV, respectively, for the surface and depth layers. Background correction and peak fitting procedures were performed using CASA XPS software.

3. Basic theory of spectroscopic ellipsometer

Ellipsometer is principally based on the change in polarization state during reflection off of a light from a film surface at an oblique angle of incidence, φ [13,14]. The incident light at the planar interface is defined with an optical plane wave:

$$E = E_{inc} = E_{p,inc} + E_{s,inc} \tag{1}$$

The amplitude ratio of reflection coefficients in terms of optical plane wave components are given as;

$$r_p = \frac{E_{p,refl}}{E_{p,inc}} \quad \text{and} \quad r_s = \frac{E_{s,refl}}{E_{s,inc}} \tag{2}$$

Complex reflection ratio, ρ, is obtained as an outcome of matching the electric and magnetic fields at the interface between different materials;

$$\rho = \frac{r_p}{r_s} = \frac{|r_p|}{|r_s|} e^{i(\delta_p - \delta_s)} = \tan \Psi e^{i\Delta} \tag{3}$$

where ψ, Δ and ρ are the parameters of an ellipsometer measurement.

Furthermore, complex refractive index, $N = n + ik$, and dielectric constant, $\varepsilon = \varepsilon_1 + i\varepsilon_2$, describe the optical properties of any medium. n and k are called the refractive index and extinction coefficient, respectively. Relations between real and imaginary parts of complex refractive index and dielectric constant are given by:

$$\varepsilon_1 = n^2 - k^2 \quad \text{and} \quad \varepsilon_2 = 2nk \tag{4}$$

$$k = \frac{\lambda}{4\pi} \alpha \tag{5}$$

$$I(x) = I_o e^{-\alpha x} \tag{6}$$

where α is absorption coefficient of material, and I is intensity of light in the dielectric material from which light is passing through. The 5 parameters, n, k, ε_1, ε_2 and α define the optical characteristics and they are, in the mean time, related to the electronic properties of the medium.

The relation between optical and electrical parameters of bulk materials [14] is found as:

$$\varepsilon = \varepsilon_1 + i\varepsilon_2 = \sin^2\varphi \left[1 + \tan^2\varphi \left(\frac{1 - \rho}{1 + \rho} \right)^2 \right] \tag{7}$$

4. Results and discussion

4.1. FTIR spectra of DC sputtered HfO_2 films

Fig. 2 shows FTIR spectra of Hf oxide films grown at 100, 150, and 200 °C for 5 min with O_2/Ar gas ratio of 0.4 applying 30 W of DC

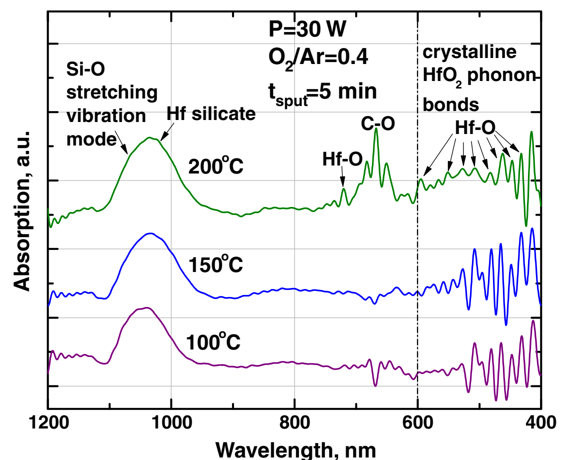

Fig. 2. FTIR spectra obtained from Hf oxide films grown at 100, 150, and 200 °C with O_2/Ar gas ratio of 0.4 for 5 min at 30 W of DC sputtering power.

sputtering power. The spectra were taken between 400 and 1200 cm^{-1}, since the low wavenumber region (<1100 cm^{-1}) is more important for detection of hafnium-oxide-related bonds.

It is clearly observed for all three substrate temperatures that not only broad but also very intense absorption band standing between 950 and 1120 cm^{-1} can be decomposed into two intensive peaks located at the vicinity of 1070 and 1020 cm^{-1} corresponding, respectively, to Si–O stretching vibration mode and hafnium silicate ($HfSi_xO_y$) [15]. The total broad-band peak's intensity increases as well as a slight shift to lower wavenumber regions as a result of substrate temperature increments ranging from 100 to 200 °C is realized. Since the peak intensity reflects the film thickness, it can be deduced that the thickness of hafnium silicate layer increases when the substrate temperature is increased. Having very close location but not at the expected exact position of natural oxide of SiO_2 (1075 cm^{-1}), however, implies that this interfacial oxide layer is in the form of suboxide of Si, i.e. SiO_x with x<2, instead of natural oxide form [6]. A slight shift to lower wavenumber region corresponds to transforming of natural SiO_2 interfacial layer to suboxide form of Si as a result of substrate temperature increments.

The main FTIR peaks reflecting Hf–O bonds are getting recognized well when the substrate temperature increases. It is given in the literature that the main peaks around 595, 551, 527, 507 cm^{-1} are due to Hf–O chemical bonds, so does 720 cm^{-1} one [16,17]. It is obvious from the figure that 720 cm^{-1} peak is only recognized in 200 °C grown film, while not even definite with lower substrate temperature ones. Therefore, it can be commented on this reality that Hf–O chemical bonds are not even traced when growth process takes place below 200 °C substrate temperature. It is reported also that the presence of sharp HfO_2 phonon bonds in the low wavenumber region (600–400 cm^{-1}) is the result of crystalline structure of the grown films [18]. Since these defined peaks between 400 and 600 cm^{-1} are well captured in 200 °C substrate temperature grown film, we can comment that not only Hf–O phonon bonds recognized when the substrate temperature increases but also the crystallization occurs at the same time.

Even though the most intensive features of HfO_2 are reported in the 100–500 cm^{-1} region, most of which extend outside of our measurement range (lower than 400 cm^{-1}) [17].

Since FTIR measurement was done in air, as a result, the C–O vibration mode is detected as well at 670 cm^{-1} of its expected position [19].

4.2. XRD structural properties

XRD spectra obtained from Hf oxide films grown at 100, 150, and 200 °C with O_2/Ar gas ratio of 0.4 for 5 min at 30 W of DC sputtering power is plotted in Fig. 3. X-ray diffraction (XRD) of HfO_2 sputter grown films on *p*-type (100) Si with natural SiO_2 oxide was performed at room temperature in the measurement range for 2θ from 10 to 65°.

It is obvious that the film grown at 100 °C is mainly amorphous while a very tiny poly-crystalline structure starts to be recognized for HfO_2. Its intensity increases very tiny for 150 °C, while it is recognizable enough at 200 °C substrate temperature grown film. This peak observed around 28° of 2θ attributed to (111) monoclinic phase of HfO_2 [17,20–23]. Nevertheless, having a low peak intensity and high FWHM value, it can be inferred that the microcrystalline structure has just been started to be formed. Pereira et al. studied the sputter grown HfO_2 thin film's structural analysis using XRD with respect to substrate temperature during growth from the room temperature to 200 °C [20]. Even though amorphous structure was detected at room temperature growth process, they also recognized a peak around 28° for 2θ when the substrate temperature was increased to 200 °C.

The other two intensive peaks around 33.3° and 62.1° in Fig. 3 are the signals coming from the Si (100) substrate underlying thin hafnium oxide film. This microcrystalline structure of HfO_2 film grown

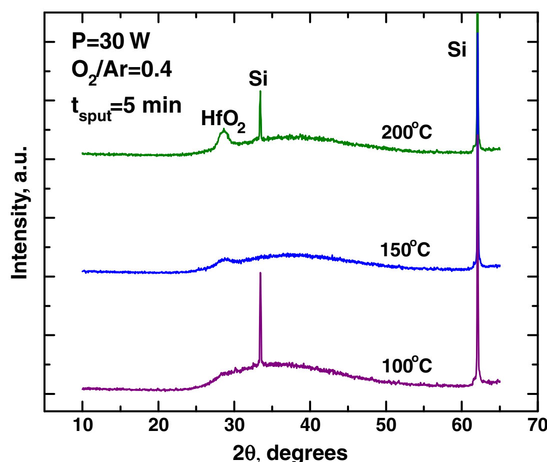

Fig. 3. XRD spectra obtained from Hf oxide films grown at 100, 150, and 200 °C with O_2/Ar gas ratio of 0.4 for 5 min at 30 W of DC sputtering power.

at 200 °C can also be predicted from the sharpness of phonon spectrum in the 400 to 600 cm^{-1} region of FTIR spectrum as seen in Fig. 2 [18].

4.3. XPS depth profiling spectrum for chemical analyses

XPS depth profiling spectra obtained from Hf oxide film grown at 200 °C with O_2/Ar gas ratio of 0.4 for 5 min at 30 W of DC sputtering power are shown in Fig. 4(a) for Hf 4*f* and (b) for Si 2*p* spectrum. It is obvious from Fig. 4(a) that all levels containing hafnium-oxide can be decomposed into two main peaks. This situation for HfO_2 is explained as a spin-orbit splitting of 1.6 eV at 16.90 and 18.50 eV, respectively, for Hf $4f_{7/2}$ and Hf $4f_{5/2}$ [6]. Nevertheless, these peaks, in the vicinity of Si, shift to higher binding energies, i.e. 17–17.5 eV, for Hf $4f_{7/2,}$ which can be attributed to $HfSi_xO_y$. It can be inferred that the peaks corresponding to initial etching cycles belong to HfO_2 mode, while the peaks start to be shifting to higher binding energy side after the 5th etching cycle. Therefore, it is clear and also supported by the FTIR spectra (Fig. 2) that $HfSi_xO_y$ mode is effective for a thick layer until around 10th etching cycle. Then, the peaks again start to be shown around the position corresponding to HfO_2 mode and last until the substrate is reached.

Kirsch et al. pointed out two extra features at 15.0 and 16.6 eV in Hf 4f XPS spectra. They concluded that these small shoulders correspond to Hf–Si bonding [24]. Similarly, Fang et al. declared that the Hf 4f peak shifted to lower binding energy as well as an additional feature appeared at 14.85 eV corresponding to Hf–Si bonds at the interface [25]. It is clear from Fig. 4(a) that these shoulder like peaks in Hf 4f spectra do not exist in this study. Therefore, it can be concluded that there is no indication for the presence of $HfSi_x$.

XPS depth profile of Si 2*p* signals of reactively sputtered Hf-oxide film on (100) *p*-Si substrate with native oxide is given in Fig. 4(b). It is well known that the signals obtained around 99.3 eV is the result of elemental (metallic) Si (Si^0), while the higher binding energies till around 104 eV correspond to the oxidation states of Si. From these, however, the lower binding energy ones closer to the metallic Si are suboxides, and the highest energy one corresponds to the Si^{4+} [2]. It is seen that elemental Si^0 is started to be seen at the very surface layers, i.e. starting from the 4th etching cycle and continuing till the depth of the oxide having its intensity getting lowered but at a detectable level. However, after some level of depth like 10th etching cycle, it started to be increased again gradually reaching to the same intensity levels of oxide form of Si, i.e. SiO_x and being dominant mode after the 12th cycle. Therefore, it can be inferred from XPS depth profiling, as well as confirmed with ellipsometric analysis, that there is a very broad interfacial oxide region since the substrate is reached after the 17th etching cycle of XPS spectra. This behavior of having a reasonable amount of elemental Si very close to the top layers of grown hafnium

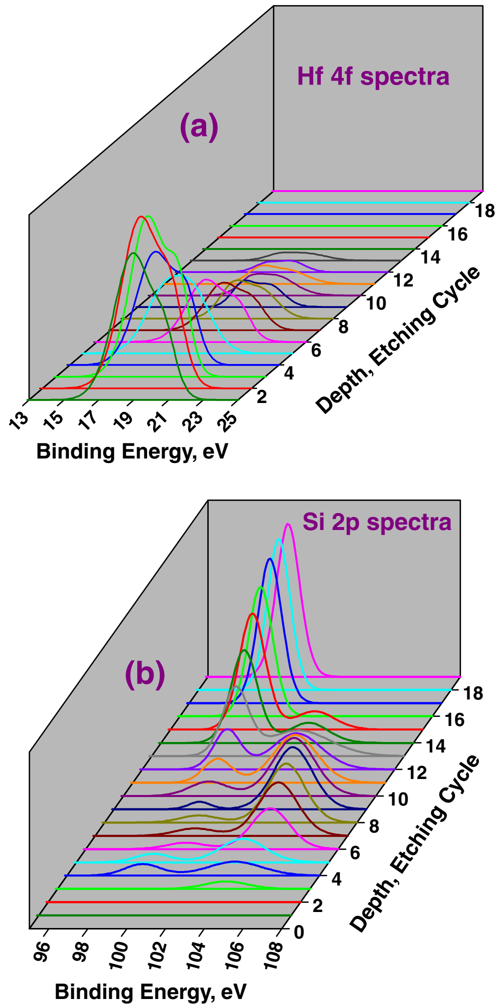

Fig. 4. XPS depth profiling spectra for (a) Hf 4*f*, (b) Si 2*p*.

oxide film gives the idea of causing elementally active sputtered Hf radicals decompose the native SiO_2 to form elemental silicon atom and oxygen molecule and/or atom explicitly. As a result, the oxygen gained from the native SiO_2 oxide is used to form HfO_2 while leaving unbonded elemental Si atoms or Si-suboxide behind [3].

4.4. SE optical properties

4.4.1. Substrate temperature effect

SE measurements with respect to wavelength over the used spectral range of 300–850 nm at 70° incidence angle of light on HfO_2 film grown on *p*-Si (100) were made under vacuum conditions. Sputtered grown HfO_2 film on Si substrate was modeled as Air/HfO_2-film/SiO_2/c-Si(100). Thickness and refractive index of HfO_2 film as well as thickness of SiO_2 film were left as variable for fitting process. Then, the constructed model was fitted for HfO_2 thin film using Cauchy dispersion relation, since HfO_2 is transparent in the spectral range of interest, i.e. $\lambda > 350$ nm. The equations for Cauchy dispersion model are,

$$n(\lambda) = n_0 + C_0 \frac{n_1}{\lambda^2} + C_1 \frac{n_2}{\lambda^4} \quad (8)$$

$$k(\lambda) = k_0 + C_0 \frac{k_1}{\lambda^2} + C_1 \frac{k_2}{\lambda^4} \quad (9)$$

where $C_0 = 10^2$ and $C_1 = 10^7$ with λ is in units of *nm* with n_0, n_1, n_2, k_0, k_1, k_2 are numbers to be fitted with respect to wavelength.

Fig. 5 shows the substrate temperature effect during growth on refractive indices of sputter grown films. These films were grown under the conditions of 30 W of DC sputter power, O_2/Ar gas ratio of 0.4 and 5 min sputtering time. Refractive index with respect to SE wavelength ranging from 300 to 850 nm was measured for the substrate temperatures of 100, 150 and 200 °C. It is seen from Table 1(a) that there is a highly positive effect of substrate temperature increments on refractive index increments of grown HfO_2 film. It should be realized that this effect is even much more emphasized for higher substrate temperatures. The refractive index of grown hafnium-oxide layer is obtained as 1.54 for 100 °C, while it increases 1.68 for 150 °C at the wavelength of 632.8 nm. Furthermore, the measured refractive index as being 1.83 for the films grown at 200 °C is the one closest to that of bulk HfO_2 value, i.e. 2.1, at 632.8 nm. Therefore, the results infer us that the highest substrate temperature choice used in our experiments, i.e. 200 °C, results in the best refractive index spectra obtained for DC sputtered grown films.

4.4.2. Oxygen to argon gas ratio effect

Fig. 6 shows the O_2/Ar gas ratio effect on refractive index for the wavelength range from 300 to 850 nm of sputter grown films. These films were grown under the conditions of 30 W, 200 °C and 5 min, respectively, for DC sputtering power, substrate temperature and sputtering time. It is detected that the refractive index value at 632.8 nm wavelength increases when O_2/Ar gas ratio decreases. Refractive index values of grown Hf-oxide films at the wavelength of 632.8 nm are obtained as 1.79, 1.83, 1.85 for O_2/Ar gas ratio values, respectively, of 0.5, 0.4, 0.2. Therefore, the results show us that the refractive index values increase depending inversely on oxygen gas amount inside the vacuum system, and the lowest used oxygen to argon gas ratio of 0.2 gives the best refractive index values obtained for DC sputter grown hafnium-oxide films.

The more probable reason of why the refractive index of grown Hf-oxide film gets increased when the O_2/Ar ratio gets lowered could be best described with a following explanation: Since the increased amount of oxygen gas in the vacuum chamber results in an increment of the scattering centers of sputtered Hf atoms, therefore, some part of Hf atoms are prevented from reaching to the substrate. Additionally, when the oxygen quantity in the O_2/Ar ratio is increased, then oxygen diffusion into the interfacial region increases resulting in an undesired interfacial layer formation between the high-κ thin film and Si substrate. Similar results can also be detected from the literature that, not only the oxygen diffusion rate increases but the growth rate of HfO_2 film is decreased at high levels of oxygen concentrations [20]. Therefore, the increased amount of oxygen

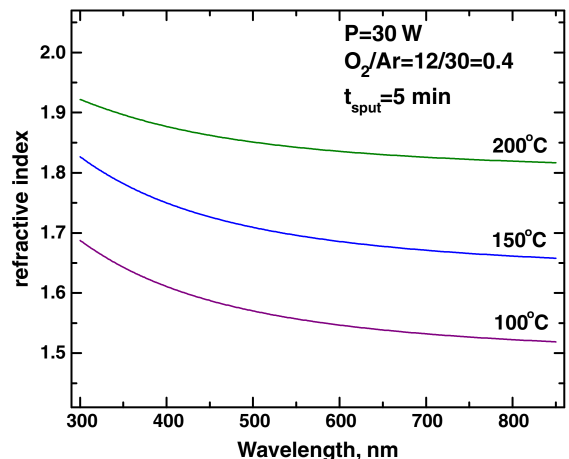

Fig. 5. Substrate temperature effect on refractive index of DC sputter grown hafnium-oxide films.

Table 1
SE fitting results given at the wavelength of 632.8 nm for; (a) 30 W sputter power for 5 min at the gas ratio of 0.4, (b) 0.2 gas ratio at the substrate temperature of 200 °C for 5 min.

(a)

Substrate temperature °C	Layer property	Thickness (d) nm	Refractive index (n)
100	HfO_2	17.70	1.54
	Silicon-oxide	5.87	–
150	HfO_2	14.83	1.68
	Silicon-oxide	10.45	–
200	HfO_2	16.13	1.83
	Silicon-oxide	11.55	–

(b)

Sputter power Watt	Layer property	Thickness (d) nm	Refractive index (n)
20	HfO_2	16.62	1.70
	Silicon-oxide	3.57	–
25	HfO_2	11.82	1.72
	Silicon-oxide	12.96	–
30	HfO_2	15.59	1.85
	Silicon-oxide	12.66	–

ratio affects the evolution of hafnium-oxide film in a negative manner, i.e. resulting in a porous film structure as well as an uncontrollable interfacial layer formation. As a result, the oxidation process is obtained as more effective at lower oxygen contents compared to those of higher oxygen contents. The future task would be to obtain the characteristics of grown HfO_2 film for O_2/Ar gas ratio of lower than 0.2.

4.4.3. Sputter power effect

Fig. 7 shows the sputter power effect on the refractive index values of sputter grown films in the wavelength range from 300 to 850 nm. These films were grown under the conditions of 200 °C, 0.2, 5 min, respectively, for substrate temperature, oxygen to argon gas ratio and sputtering time. Refractive index and thickness values of layers at the wavelength of 632.8 nm, respectively, for 20, 25, and 30 W DC sputter powers are given in Table 1(b). It is obvious that the refractive index values of hafnium-oxide films grown under the sputter powers of 20 and 25 W are too much lower than that of bulk value of HfO_2. However, having been a value of 1.85, the refractive index for 30 W is very close to that of bulk HfO_2. It can be concluded that DC sputter power of 30 W is a threshold to produce hafnium oxide films whose

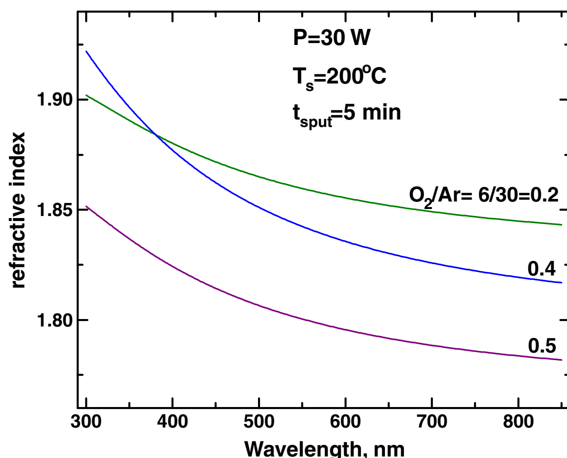

Fig. 6. Oxygen to argon gas ratio effect on refractive index of DC sputter grown hafnium-oxide films.

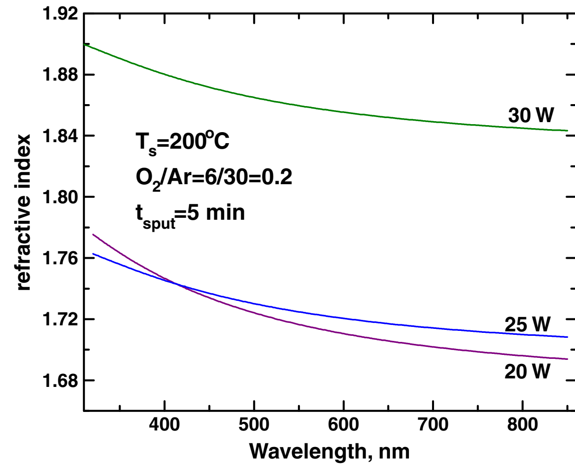

Fig. 7. Sputter power effect on the refractive index of DC sputter grown hafnium-oxide films.

density is being close to that of bulk HfO_2. Moreover, DC sputtering power values should be around 30 W and/or little more to grow dense enough hafnium-oxide films.

5. Conclusion

HfO_2/SiO_2/p-Si (100) stacks were studied in terms of structural and optical analyses by means of FTIR, XRD, XPS depth profiling and Spectroscopic Ellipsometry. FTIR for structural and bonding analyses as well as XRD for crystalline structural analyses were studied for Hf oxide films grown at 100, 150, and 200 °C with O_2/Ar gas ratio of 0.4 for 5 min at 30 W of DC sputtering power. FTIR analyzing technique confirms that the films grown at 200 °C have better results in terms of having definite Hf–O structural bondings, however, the films grown at lower substrate temperatures do not have the explicit peaks decisive to HfO_2 films. XRD results of the same property films with FTIR analyzing technique show that the films have amorphous structure grown at the substrate temperature of 100 °C, while the polycrystalline structure starts to be seen around 150 °C and it increases little more for films grown at the substrate temperature of 200 °C.

The FTIR, XRD and SE results with respect to substrate temperatures show us that when the substrate temperature gets lowered, then the grown HfO_2 film is mainly amorphous. Its intensity increases very tiny for 150 °C, while it is recognizable enough at 200 °C. Additionally, the main FTIR peaks reflecting Hf–O bonds are recognized well when the substrate temperature increases, however, the crystallization is detected at the same time. From SE measurements, a highly positive effect of substrate temperature increments on refractive index increments of grown film is detected. However, refractive index is getting extremely low, i.e. 1.54 at 632.8 nm, for 100 °C substrate temperature case. Even though the refractive index is increased for the choice of 200 °C substrate temperature, the crystalline structure for grown HfO_2 film is detected from not only XRD but also SE measurements. Since the crystalline structure for high-κ films is not a desired property, the substrate temperature was restricted to be at 200 °C. However, for a future task, the substrate temperature higher than 200 °C can be studied in order to obtain the optical as well as structural properties of grown film.

XPS depth profiling spectra were studied for the Hf oxide film grown at 200 °C with O_2/Ar gas ratio of 0.4 for 5 min at 30 W of DC sputtering power. The results show us that there is an extremely thin HfO_2 layer on top of a respectively broad interfacial layer formed mainly from Si suboxide and Hf-silicate. It is clearly explained by an XPS depth profiling spectra that the formation of $HfSi_x$ was eliminated since there is no direct contact of sputtered Hf with SiO_2/Si substrate.

The results infer that there existed a very thin perfect Hf-oxide layer, later Si–Si bonds are detected even before Si suboxide layer is reached and then Si substrate is reached. Since Si–Si bonds were measured just before Si-oxide is reached, it can be realized that highly reactive sputtered Hf atoms consume some of the oxygen atoms from the underlying SiO_2 to form hafnium-oxide by leaving Si–Si bonds behind [3]. Our results also confirm what Yamamoto et al. revealed with their experiment that the oxygen radicals oxidize the Hf metal more selectively than Si substrate [11].

Finally, we have additionally obtained the best oxidation conditions for Hf-oxide films in terms of SE optical analyzing technique overall the used physical growth parameters, i.e. substrate temperature, oxygen to argon gas ratio, and DC sputtering power. The SE optical analyzing technique results in 200 °C, 0.2, and 30 W respectively for the substrate temperature, oxygen to argon gas ratio and DC sputtering power as the best oxidation conditions from the overall used parameters.

Acknowledgements

This research was supported mainly by The Scientific and Technological Research Council of Turkey (TUBITAK) with project number of 107T117 and partially by Izmir Institute of Technology with research project number of 2008 IYTE 37.

References

[1] G.D. Wilk, R.M. Wallace, J.M. Anthony, J. Appl. Phys. 89 (2001) 5243.
[2] G. Aygun, E. Atanassova, K. Kostov, R. Turan, J. Non-Cryst. Solids 352 (2006) 3134.
[3] G. Aygun, I. Yildiz, J. Appl. Phys. 106 (2009) 014312.
[4] G. Aygun, R. Turan, Thin Solid Films 517 (2008) 994.
[5] S. Hayashi, K. Yamamoto, Y. Harada, R. Mitsuhashi, K. Eriguchi, M. Kubota, M. Niwa, Appl. Surf. Sci. 216 (2003) 228.
[6] Q. Fang, J.-Y. Zhang, Z. Wang, M. Modreanu, B.J. O'Sullivan, P.K. Hurley, T.L. Leedham, D. Hywel, M.A. Audier, C. Jimenez, J.-P. Senateur, I.W. Boyd, Thin Solid Films 453–454 (2004) 203.
[7] R. Thielsch, A. Gatto, J. Heber, N. Kraiser, Thin Solid Films 410 (2002) 86.
[8] J. Kim, S. Kim, H. Kang, J. Choi, H. Jeon, M. Cho, K. Chung, S. Back, K. Yoo, C. Bae, J. Appl. Phys. 98 (2005) 094504.
[9] J. Zhu, Z.G. Liu, Y. Feng, J. Phys. D Appl. Phys. 36 (2003) 3051.
[10] G. Aygun, E. Atanassova, A. Alacakir, L. Ozyuzer, R. Turan, J. Phys. D Appl. Phys. 37 (2004) 1569.
[11] K. Yamamoto, S. Hayashi, M. Niwa, M. Asai, S. Horii, H. Miya, Appl. Phys. Lett. 83 (2003) 2229.
[12] R. Tan, Y. Azuma, I. Kojima, Appl. Surf. Sci. 222 (2004) 346.
[13] H.G. Tompkins, W.A. McGahan, Spectroscopic Ellipsometry and Reflectometry, John Wiley and Sons, New York, 1999.
[14] H. Fujiwara, Spectroscopic Ellipsometry: Principles and Applications, John Wiley & Sons, England, 2007.
[15] G. He, L.D. Zhang, Q. Fang, J. Appl. Phys. 100 (2006) 083517.
[16] T.C. Chen, C.Y. Peng, C.H. Tseng, M.H. Liao, M.H. Chen, C.I. Wu, M.Y. Chern, P.J. Tzeng, C.W. Liu, IEEE Trans. Electron Devices 54 (2007) 759.
[17] D.A. Neumayer, E. Cartier, J. Appl. Phys. 90 (2001) 1801.
[18] A. Deshpande, R. Inman, G. Jursich, C. Takoudis, Microelectron. Eng. 83 (2006) 547.
[19] E. Atanassova, G. Aygun, R. Turan, Tz. Babeva, J. Vac. Sci. Technol. A 24 (2006) 206.
[20] L. Pereia, A. Marques, H. Aguas, N. Nedev, S. Georgiev, E. Fortuna, R. Martins, Mater. Sci. Eng. B 109 (2004) 89.
[21] S.W. Nam, J.H. Yoo, S. Nam, H.J. Choi, D. Lee, D.H. Ko, J.H. Moon, J.H. Ku, S. Choi, J. Non-Cryst. Solids 303 (2002) 139.
[22] G. He, M. Liu, L.Q. Zhu, M. Chang, Q. Fang, L.D. Zhang, Surf. Sci. 576 (2005) 67.
[23] G. Tian, S. Wu, K. Shu, L. Qin, J. Shao, Appl. Surf. Sci. 253 (2007) 8782.
[24] P.D. Kirsch, C.S. Kang, J. Lozano, J.C. Lee, J.G. Ekerdt, J. Appl. Phys. 91 (2002) 4353.
[25] Q. Fang, J.Y. Zhang, Z. Wang, M. Modreanu, B.J. O'Sullivan, P.K. Hurley, T.L. Leedham, D. Hywel, M.A. Audier, C. Jimenez, J.P. Senateur, Ian W. Boyd, Thin Solid Films 453–454 (2004) 203.